CHAPTER 2

BASIC CONCEPTS

With the ever more detailed and profound observations of the universe, we have become exposed to a vast field of coronal phenomena in the formation, activity, and late phases of stars. However, coronal physics poses some unexpected, recondite difficulties to the beginner and to the uninitiated astronomer in particular. The fundamental principles are simple: Maxwell's equation of electrodynamics and Boltzmann's equation of statistical mechanics (Chapter 1). On the other hand, the complexity of plasma phenomena is bewildering. The pioneers of plasma physics have had similar experiences; they have subdued some of the problems with elegant approximations, clever tricks, and deep insights. Their ideas have been checked in the laboratory, the solar wind and the magnetosphere, and the results have initiated new developments. The beginner should try to understand the fundamental concepts and the range of their applicability, even if they later seem to be outshone by brilliant mathematics or covered up by cumbersome algebra.

2.1. Single Particle Orbit

It will be shown in Section 2.6 that the collision time increases with particle velocity. Therefore, the assumption of a single particle moving in a vacuum, permeated by magnetic and electric fields, is particularly relevant for energetic particles, which can reach large distances before being deflected by collisions with the thermal background particles. In other words, they feel primarily the large scale electric and magnetic fields created by background particles, but have little stochastic interactions with individual particles.

The orbit of just one single particle in time-varying, spatially inhomogeneous electromagnetic fields is already a problem of considerable complexity. In this section we only consider the more elementary principles.

2.1.1. Homogeneous Magnetic Field

Magnetic fields are ubiquitous in stellar coronae (Figure 1.2). The fields are related to currents driven by sub-photospheric motions. Hindered by the high conductivity of a plasma atmosphere, coronal magnetic fields can change only slowly. The field lines guide the motion of charged particles and have an important physical meaning.

Let us start with a particle moving in a stationary, homogeneous magnetic field. We assume that no other charges and fields interact with our particle. The equation of motion (1.4.1) then reduces to

$$\frac{\partial(m\gamma\mathbf{v})}{\partial t} = \frac{q}{c}(\mathbf{v}\times\mathbf{B}) \quad . \tag{2.1.1}$$

As the Lorentz force is perpendicular to the velocity, the motion can be regarded as a superposition of a circular orbit perpendicular to the magnetic field and a straight, inertial movement parallel to the field. The circular motion is called *gyration*. The gyroradius R follows immediately from Equation (2.1.1),

$$R = \frac{m\gamma c}{|q|B}\, v_\perp \quad , \tag{2.1.2}$$

which we define more generally as a vector,

$$\mathbf{R} := -\frac{mc\gamma}{qB^2}(\mathbf{v}\times\mathbf{B}) \quad . \tag{2.1.3}$$

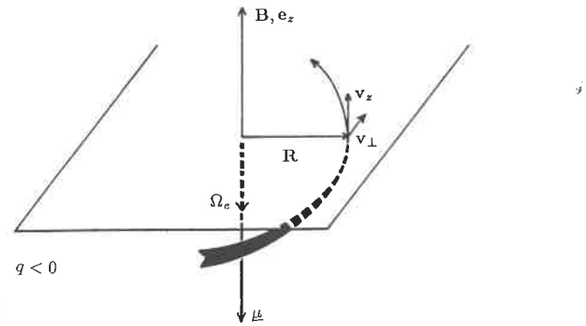

Fig. 2.1. The orbit of an electron in a homogeneous magnetic field.

The subscripts $\perp$ and z denote components perpendicular and parallel to the magnetic field, respectively. Throughout the book the local coordinates are chosen such that the z-axis is parallel to $\mathbf{B}$.

The gyration resulting from Equation (2.1.1) is counterclockwise for a positive charge when viewed along $\mathbf{B}$, and clockwise for an electron. As a consequence, the radius vector $\mathbf{R}$ always points from the center of the circular motion to the particle, independently of the sign of q. Furthermore, the gyrofrequency is defined in vector notation as

$$\boldsymbol{\Omega} := \frac{q}{m\gamma c}\mathbf{B} \quad . \tag{2.1.4}$$

In this chapter we limit ourselves to non-relativistic phenomena, and we shall put $\gamma = 1$ in the following. We note that the gyrofrequency (Eq. 2.1.4) then becomes

independent of velocity and equal for all particles of a species. The gyrofrequencies of the various species are characteristics of a plasma and will play an important role in the theory of waves (Chapter 4). In Equations (2.1.3) and (2.1.4) vectors have been defined to simplify the mathematics later. They are drawn in Figure 2.1, which depicts the spiraling orbit of an electron, the combination of parallel and circular motion.

No work is done by the Lorentz force, as it is perpendicular to the orbit. An important result of the gyration is the electric ring current due to the circular motion of the particle. It is charge per time, thus

$$< I >= \frac{|q\Omega|}{2\pi} \quad . \tag{2.1.5}$$

This ring current is the cause of a magnetic moment of a particle defined by

$$\underline{\mu} := \frac{q}{2c}(\mathbf{R} \times \mathbf{v}_\perp) \quad . \tag{2.1.6}$$

Its absolute value is

$$\mu = \frac{\pi R^2}{c} < I > = \frac{\frac{1}{2}mv_\perp^2}{B} \quad . \tag{2.1.7}$$

The magnetic moment induces a secondary magnetic field, $\mathbf{B}^{\text{ind}}$, which has the form of a dipole in the far field (at distances $r \gg R$). For example, in the axis of the particle orbit, the induced field has the value $\mathbf{B}^{\text{ind}} = 2\underline{\mu}r^{-3}$. There are two important points to note in Equation (2.1.6):

- The magnetic moments of positive and negative charges are pointing in the same direction. The induced magnetic fields of all particles add constructively.
- The directions of $\mathbf{B}^{\text{ind}}$ and $\mathbf{B}$ are antiparallel. The induced field counteracts the primary field and reduces the total field in the plasma. This diamagnetism of a plasma has far-reaching consequences (see example below).

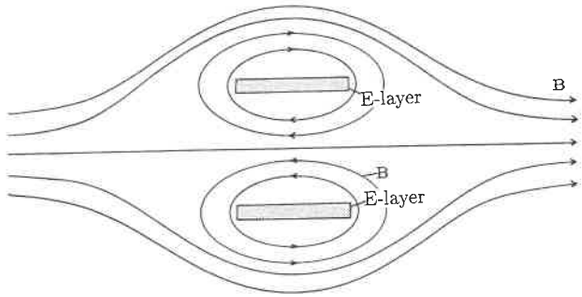

Fig. 2.2. Monoenergetic electrons accelerated in a magnetic field form a cylindrical shell (called E-layer, shaded) and deform the field.

The Astron machine in fusion research may serve as an illustration (Fig. 2.2). Energetic electrons are injected into initially parallel magnetic field lines. These electrons circle in a cylindrical shell, termed the E-layer. Their diamagnetism reduces the field inside the E-layer and adds to the field outside. Thus the magnetic field forms a 'magnetic bottle', shown in Section 2.2, which is suitable for confinement. The Astron configuration makes use of the diamagnetism of the injected electrons to confine ions. Heating or acceleration of particles in coronal loops may lead to similar effects.

2.1.2. Inhomogeneous Magnetic Field

We now look at a particle in a converging magnetic field as sketched in Figure 2.3. Similar field geometries may exist near the footpoints of coronal loops or in the polar regions of stars and planets. The magnetic field at the particle's instantaneous position can be decomposed into a component, $\mathbf{B}_z$, parallel to the field at the center of the gyration, and a perpendicular component, $\mathbf{B}_r$. The Lorentz force on the particle can also be written in two components:

$$\mathbf{F}_{L,r} = \frac{q}{c}(\mathbf{v}_\perp \times \mathbf{B}_z) \quad , \tag{2.1.8}$$

$$\mathbf{F}_{L,z} = \frac{q}{c}(\mathbf{v}_\perp \times \mathbf{B}_r) \quad . \tag{2.1.9}$$

The first, Equation (2.1.8), is the radial force component analogous to the homogeneous case. Equation (2.1.9) describes a force along the axis of the spiraling particle motion. It can be evaluated from $\nabla \cdot \mathbf{B} = 0$ (Eq. 1.4.4), which in cylindrical coordinates becomes:

$$\frac{1}{r}\frac{\partial}{\partial r}(rB_r) + \frac{\partial B_z}{\partial z} = 0 \quad . \tag{2.1.10}$$

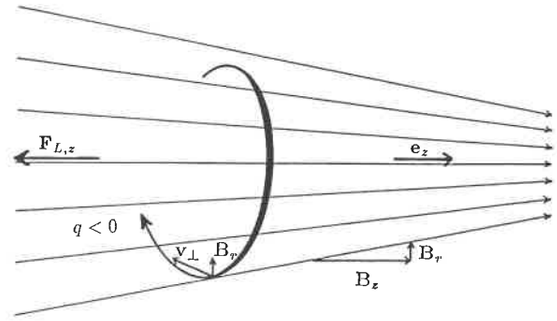

Fig. 2.3. Particle motion in a converging magnetic field produces a Lorentz force $\mathbf{F}_{L,z}$ in the opposite direction.

Let us consider the case where r is much smaller than the scale length of the derivative of B_z ($r \ll |B_z'/(\partial B_z'/\partial r)|$, where $B_z' := \partial B_z/\partial z$). In such a mildly inhomogeneous field, Equation (2.1.10) can be integrated approximately to

$$B_r \approx -\frac{1}{2} r \frac{\partial B_z}{\partial z} \quad . \tag{2.1.11}$$

Inserting in the gyroradius (Eq. 2.1.2) for r, Equation (2.1.9) yields

$$F_{L,z} = -\mu \frac{\partial B_z}{\partial z} \quad . \tag{2.1.12}$$

For example, $\partial B_z/\partial z > 0$ (a converging field as in Fig. 2.3) produces an F_z in the negative z-direction. It slows down the parallel velocity of a particle moving along the converging field and can reflect the particle into the opposite direction. In Section 2.2 we shall take a first look at the possibility of trapping particles by such 'magnetic mirrors'.

2.1.3. Conservation of the magnetic moment

We shall show in this section that in a mildly inhomogeneous, stationary magnetic field the magnetic moment of a particle is a constant of motion. It is generally sufficient to require that $|(\mathbf{R} \cdot \nabla)\mathbf{B}| \ll |\mathbf{B}|$ and $B_r \ll B_z$. We neglect collisions, electric fields and other forces. With $F_z = m\dot{v}_z$ we derive from Equation (2.1.12) the rate of change of the parallel energy component,

$$m v_z \dot{v}_z = -\mu \frac{\partial B}{\partial z}\frac{dz}{dt} = -\mu \frac{dB}{dt} \quad . \tag{2.1.13}$$

The forces are evidently perpendicular to the velocity components (Eqs. 2.1.8 and 2.1.9); thus the particle energy is conserved,

$$\frac{d}{dt}\left(\frac{1}{2}mv_z^2 + \frac{1}{2}mv_\perp^2\right) = 0 \quad . \tag{2.1.14}$$

Inserting (2.1.7) and (2.1.13), one obtains

$$-\mu \frac{dB}{dt} + \frac{d}{dt}(\mu B) = 0 \quad . \tag{2.1.15}$$

Since $B \neq 0$ by assumption, it immediately follows that

$$\frac{d\mu}{dt} = 0 \quad . \tag{2.1.16}$$

It is also instructive to consider the conservation of the magnetic moment from a different point of view. Since the transverse motion is periodic, an action integral $\mathcal{J} = \int p_\perp ds_\perp$ can be defined, where $p_\perp$ is the transverse momentum and $ds_\perp$ is the perpendicular component of the gyration path. It is easy to show that $p_\perp$ and $s_\perp$ satisfy the conditions of canonical coordinates. The integration is over a

complete cycle of $s_\perp$, i.e. over one gyration. The action integral for the transverse part of the motion is

$$\mathcal{J} = \frac{4\pi mc}{q}\mu \quad . \tag{2.1.17}$$

Theoretical mechanics proves that, if a system changes slowly compared to the period of motion (and is not in phase with the period), an action integral remains constant. Such a variation of a system is termed *adiabatic*, and action integrals become *adiabatic invariants*.

In our case the system consists of the magnetic field and the particle. If the particle moves through a region where the magnetic field varies slowly, Equation (2.1.17) confirms that the magnetic moment is conserved. In addition to spatial variations, the magnetic moment is also conserved during temporal changes of magnetic field strength. This property can accelerate particles: Consider an increase of B, say by compression, at a rate well below the gyrofrequency. The perpendicular part of the particle energy must then increase in proportion to B according to the definition of μ (Eq. 2.1.6). Such an energy increase is generally referred to as *betatron acceleration* and will be applied in Section 10.3.3.

The magnetic moment μ is the 'most invariant' action integral of charged particles. The obvious analogue to Equation (2.1.17) for periodic motion in a magnetic mirror is the *longitudinal invariant*,

$$\mathcal{L} := p_z L \quad , \tag{2.1.18}$$

where L is the mirror length. It may be used in connection with Fermi acceleration (Section 10.3.1).

2.1.4. Particle drifts

Our next step in understanding single particle orbits is to include some other stationary force, $\mathbf{F}$, in addition to the Lorentz force of the magnetic field. As its parallel component to the magnetic field, $\mathbf{F}_z$, accelerates the particles into a direction where they are freely moving, which is trivial, we concentrate on the effect of $\mathbf{F}_\perp$. In the non-relativistic limit, the perpendicular component of Equation (2.1.1) is

$$\frac{d\mathbf{v}_\perp}{dt} = \frac{q}{mc}(\mathbf{v}_\perp \times \mathbf{B}) + \mathbf{F}_\perp/m \quad . \tag{2.1.19}$$

This is a linear, inhomogeneous, first-order differential equation in $v_\perp$. The theory of such equations prescribes that its general solution is simply the superposition of one particular solution, say $\mathbf{w}^d$, of the full equation and of the general solution, $\mathbf{u}$, of its homogeneous part (Eq. 2.1.19 without the $\mathbf{F}_\perp/m$ term). Thus

$$\mathbf{v}_\perp = \mathbf{w}^d + \mathbf{u} \quad . \tag{2.1.20}$$

Using the general vector identity (A.9),

$$\frac{(\mathbf{F}\times\mathbf{B})\times\mathbf{B}}{B^2} \equiv \frac{(\mathbf{F}_\perp\cdot\mathbf{B})\mathbf{B}-(\mathbf{B}\cdot\mathbf{B})\mathbf{F}_\perp}{B^2} = -\mathbf{F}_\perp \quad , \tag{2.1.21}$$

it can be shown that the form

$$\mathbf{w}^d = \frac{c}{q}\frac{\mathbf{F}_\perp\times\mathbf{B}}{B^2} \tag{2.1.22}$$

is a solution of Equation (2.1.19). The homogeneous equation

$$\frac{d\mathbf{u}}{dt} = \frac{q}{m\,c}(\mathbf{u}\times\mathbf{B}) \tag{2.1.23}$$

describes the action of the Lorentz force on the particle, but in the frame of reference moving with velocity $\mathbf{w}^d$. Equation (2.1.23) represents a motion without the additional force. Its solution, $\mathbf{u}$, is the circular velocity around what is called the *guiding center*. The velocity of the guiding center is simply

$$\mathbf{v}^{gc} = \mathbf{w}^d + \mathbf{v}_z \quad . \tag{2.1.24}$$

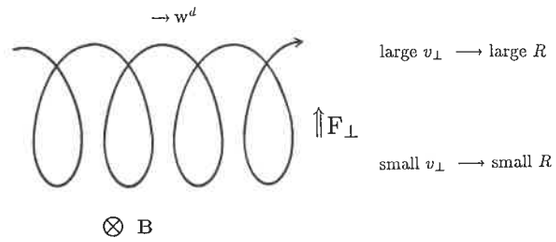

Fig. 2.4. A perpendicular force $\mathbf{F}_\perp$ on a gyrating particle causes a drift perpendicular to $\mathbf{F}_\perp$ and $\mathbf{B}$.

This tells us that the perpendicular force results in a *drift* $\mathbf{w}^d$ perpendicular to the magnetic field, in addition to the previously introduced gyration and parallel motions. The reason for this drift can be visualized in Figure 2.4. The force $\mathbf{F}_\perp$ accelerates the particle in the upward direction in Figure 2.4. It is therefore faster in the upper part of its orbit. The gyroradius increases with velocity (Eq. 2.1.2). The opposite occurs in the lower part of the figure. The effect of the variation of the gyroradius is a drift to the right (assuming a positive charge). An analogous effect, called *gradient drift*, occurs when the magnetic field strength increases in the downward direction of Figure 2.4 and reduces the gyroradius in the lower part of the orbit. In homogeneous magnetic fields and in the absence of other forces, collisionless particles are bound to a particular field line like pearls on a string. Drifts, however, can move the particles across field lines and spread them out from their original line to a larger volume. In the following, we discuss some key examples of particle drifts.

A. *Electric Field*

Let there be a stationary electric force

$$\mathbf{F}_E = q\mathbf{E} \quad . \tag{2.1.25}$$

The drift velocity resulting from Equation (2.1.22) is

$$\mathbf{w}_E = c\frac{\mathbf{E}\times\mathbf{B}}{B^2} \quad . \tag{2.1.26}$$

This is generally known as $E\times B$ drift. We note that $\mathbf{w}_E$ is independent of charge, mass, and velocity. As it is identical for all particles, the electric field can be 'transformed away' by a Lorentz transformation into a suitable frame of reference. This coordinate system moves with velocity $\mathbf{w}_E$, it is the rest frame of the $E\times B$ drifting plasma. Since $\mathbf{B}$ is perpendicular to $\mathbf{w}_E$, the magnetic field in the moving frame of reference is the same. The $E\times B$ drift can be viewed as the moving plasma carrying along its embedded magnetic field.

B. *Gravitational Field*

Let gravity be given by a gravitational acceleration $\mathbf{g}$ and

$$\mathbf{F}_g = m\mathbf{g} \quad . \tag{2.1.27}$$

According to Equation (2.1.22) it causes a drift

$$\mathbf{w}_g = \frac{mc}{q}\frac{\mathbf{g}\times\mathbf{B}}{B^2} \quad . \tag{2.1.28}$$

Note that ions and electrons drift in opposite directions. Gravitational drift produces a current! As the drift velocity, $\mathbf{w}_g$, is proportional to mass, the current consists mainly of perpendicularly moving ions. A well-known example is the ring current in the terrestrial ionosphere, where the observed ion drift velocity is of the order of 1 cm s^{-1}, in agreement with Equation (2.1.28).

C. *Curved Field Lines*

In a curved magnetic field a 'centrifugal force' may be defined, simulating the effect of particle inertia. The centrifugal drift becomes

$$\mathbf{w_c} = \frac{mc\,v_z^2}{qB^4}[\mathbf{B}\times(\mathbf{B}\cdot\nabla)\mathbf{B}] \tag{2.1.29}$$

(Exercise 2.1, below) and depends on the ratio of particle energy to charge. It has different signs for electrons and ions. The resulting current is perpendicular to the magnetic field and is directly related to the field curvature by Ampère's equation (1.4.2).

2.2. Particle Trapping in Magnetic Fields

A considerable fraction of the energy released in solar flares (estimates range from 0.1 to 50%) resides temporarily in electrons with energies far above thermal. Such particles could easily escape from the corona without collisions if they were not hindered by the magnetic field. In fact, only 0.1 to 1% of these electrons are later found in interplanetary space. This evidently reflects the predominance of loop-shaped magnetic field lines in the corona and, particularly, in active regions where flares generally occur. 'Open' field lines, which connect the active region to interplanetary space, seem to be rare or extremely well shielded from the site of acceleration. (Note that the widely used term 'open field line' is a misnomer, since in the absence of magnetic monopoles and in a finite universe all magnetic field lines must eventually close and return from space to the Sun. Nevertheless, such field lines can easily have a length exceeding the diameter of the Galaxy, and they are quantitatively different in this respect from 'closed' field lines, returning within the corona, or within about one solar radius: see Fig. 2.5)

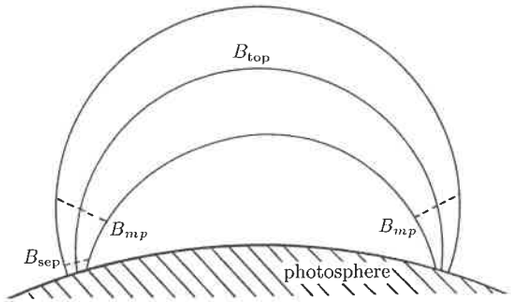

Fig. 2.5. Schematic drawing of 'closed' magnetic field lines forming loops between photospheric spots of opposite polarity.

Most energetic particles are apparently guided back to the Sun by 'closed' field lines. Some of them immediately penetrate denser plasma or even the chromosphere, where they rapidly lose their energy by collisions, emitting bremsstrahlung in hard X-rays. Others, however, remain in the corona up to several minutes, as some microwave emissions (around 3 GHz) and decimetric continuum bursts (0.3 – 3 GHz) indicate. The flare microwaves originate primarily from relativistic electrons (Section 1.2.3), and trapped electrons seem to play a role in long duration events. Decimetric continuum radiation is generally interpreted as coherent radiation of trapped electrons (Chapter 8).

Magnetic trapping can be understood as the result of conservation of the magnetic moment. The condition of smooth and only slowly varying magnetic field lines is easily satisfied in practically all we know about solar and stellar atmospheres. According to Equation (2.1.16), the magnetic moment

$$\mu = \frac{\frac{1}{2}mv_\perp^2}{B} = \text{const} \quad . \tag{2.2.1}$$

Assuming a stationary magnetic field, no work is done by the Lorentz force. Thus the particle energy is also conserved,

$$v^2 = v_\perp^2 + v_z^2 = \text{const} \quad . \tag{2.2.2}$$

Let us consider a system of looped magnetic field lines, typical of solar and stellar spots (or magnetic poles of opposite polarity), sketched in Figure 2.5. The field strength has a minimum near the top of the loop and is assumed to increase toward the photospheric footpoints. If a charged particle spirals in the direction of increasing field strength, it experiences an opposing component of the Lorentz force (given by Eq. 2.1.9), reducing v_z. This may continue until $v_z = 0$, when the particle changes the sign of its parallel velocity and is reflected. The magnetic field strength at the mirror point, B_{mp}, can readily be calculated from Equation (2.2.1),

$$B_{mp} := B_0 \left(\frac{v}{v_\perp^0} \right)^2 \quad . \tag{2.2.3}$$

The subscript 0 refers to a given point in the orbit, for instance to the top of the loop, where the particle has a perpendicular velocity component $v_\perp^0 = v_\perp^{\rm top}$. Equation (2.2.2) requires the perpendicular velocity at the mirror point to equal the initial total velocity v.

Let $B_{\rm sep}$ be the magnetic field strength at the critical height below which particles are not mirrored but lost by collisions. The altitude of the separation between collisional and collisionless behavior is somewhere in the upper chromosphere or transition region. If $B_{mp} < B_{\rm sep}$, the particle is reflected before entering the region of rapid collisions. Provided that this is also the case at the other footpoint (where the field strength may be different), the particle remains trapped in the corona. The coronal collision times are about five orders of magnitude longer than in the chromosphere (Figure 1.9, but note that super-thermal particles have a much longer collision time, as will be shown in Section 2.6). Then the particle bounces between the mirror points. The full bounce period τ in a parabolic field (like the far field of a dipole, $B = B_{\rm top}(1 + s^2/H_B^2)$, where s is the path length measured from the top of the magnetic loop), is independent of the initial parallel velocity, since the larger $v_z^{\rm top}$ is, the farther away is the mirror point. One derives

$$\tau = \frac{2\pi H_B}{v_\perp^{\rm top}} \quad . \tag{2.2.4}$$

The proof of Equation (2.2.4) is left to an exercise (2.2). The geometric parameter H_B is related to the loop length L (say from chromosphere to chromosphere) by

$$H_B \approx \frac{L/2}{\sqrt{\frac{B_{\rm sep}}{B_{\rm top}} - 1}} \quad . \tag{2.2.5}$$

B_{sep}/B_{top} is called the *mirror ratio*. It has been estimated from soft X-ray observations to be in the range of 2 – 10 for solar coronal flare loops.

If $B_{mp} \geq B_{sep}$, the particle penetrates the chromosphere and is lost from the trap. Equation (2.2.3) then states that trapping or precipitation depends only on the ratio $v/v_{\perp}^{top}$, or the particle's pitch angle, α_{top}. The pitch angle is defined by the angle of the orbit to the magnetic field,

$$\alpha_0 := \arcsin(\frac{v_{\perp}^0}{v}) \quad . \tag{2.2.6}$$

The particle is trapped if the initial pitch angle is larger than the critical value given by $\arcsin(B_{top}/B_{sep})^{1/2}$. A critical pitch angle α_c can be determined from Equation (2.2.6). It is given at every point in the loop by the local magnetic field strength B_0 and amounts to

$$\alpha_c(B_0) = \arcsin\sqrt{\frac{B_0}{B_{sep}}} \quad . \tag{2.2.7}$$

If the pitch angle is below this value, the particle will get lost with high probability before reflection.

The velocity distribution of magnetically trapped particles has characteristic cones with half-angle α_c and axes in the positive and negative v_z-directions, where the number of particles is strongly reduced. They are known as *loss-cones*. Figure 2.6 shows a typical observation of protons trapped in the Earth's dipole field with a clearly developed loss-cone. The thermal, collisional background plasma forms a nearly isotropic distribution in the center. Velocity distributions with a loss-cone can be expected whenever particles are mirrored in a converging magnetic field within less than a collision time. Particles outside of the loss-cone are trapped if their mean free path exceeds the size of the magnetic configuration. This is well-known to occur in the tenuous plasmas of planetary magnetospheres and the solar and stellar coronae, but can also be expected in the atmospheres of white dwarfs and neutron stars, in galactic magnetic fields, etc.

Loss-cone features are more than identification tags of trapped particle populations. They are an important deviation from thermal equilibrium. Even if the rest of the velocity distribution is Maxwellian, loss-cones constitute free energy. In Chapter 8 it will become clear that this free energy can be tapped by plasma instabilities causing various types of observable emission.

2.3. Generation of Beams

The previous section introduced the imprint of the magnetic field's spatial structure on the velocity distribution. Here we consider temporal changes of the distribution and study how they propagate in space. In the absence of collisions and any other forces, the particle distribution at a place $\mathbf{x}+\Delta\mathbf{x}$ and time t is determined by the distribution at $\mathbf{x}$ and $t - \Delta t$, where $\mathbf{v} = \Delta\mathbf{x}/\Delta t$ is the particle velocity. Thus

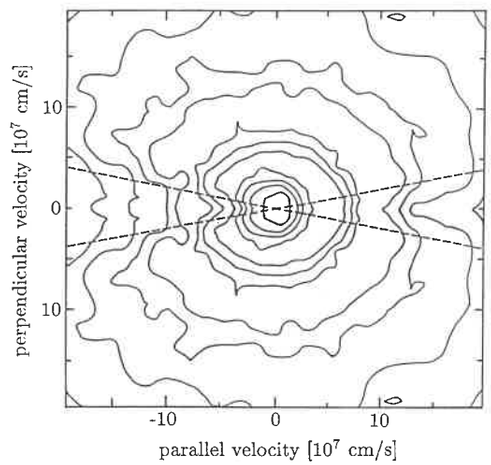

Fig. 2.6. Contour plot of proton velocity distribution observed by the VIKING satellite in the Earth's magnetosphere. The theoretical loss-cone angle given by Equation (2.2.7) is indicated (dashed). Contours are separated by a factor of 3.2 (5 dB) (after Boström, Koskinnen, and Holback, 1987).

$$f(\mathbf{x}+\mathbf{\Delta x},\mathbf{v},t) \;=\; f(\mathbf{x},\mathbf{v},t-\Delta t) \quad . \tag{2.3.1}$$

Let us use this simple model to outline the evolution of a local disturbance in velocity space. Example: Consider the rapid heating of a fraction of the particles to a temperature $T_h \gg T_c$, the temperature of the ambient medium. We take only one hot particle species for simplicity, which we assume to have a Maxwellian distribution. Since charged particles propagate along field lines (neglecting gyration and drifts), the problem can be reduced to one dimension (the z-direction). Let the number of hot particles at z_0 now increase exponentially with a time constant τ. Their distribution f at the heating site is a Maxwellian function multiplied by an exponential function,

$$f(z_0,v,t) \;=\; \frac{n_h}{\sqrt{2\pi}v_{th}} \exp\left(-v^2/2v_{th}^2\right) \cdot \exp\left(\frac{t}{\tau}\right) \quad . \tag{2.3.2}$$

With this expression, the mean thermal velocity in one velocity component and the temperature T_h are related by $v_{th} =: (k_B T_h/m)^{1/2}$ (k_B is the Boltzmann constant). The subscript t stands for thermal, h stands for the hot population. Using Equations (2.3.1) and (2.3.2) it is straightforward to derive the hot particle distribution at a site $z_0 + \Delta z$ outside the heating region from the distribution at z_0 shifted by $-\Delta t = -\Delta z/v$,

$$f(z_0 + \Delta z, v, t) = \frac{n_h e^{t/\tau}}{\sqrt{2\pi} v_{th}} \exp\left(-v^2/2v_{th}^2 - \frac{\Delta z}{v\tau}\right) \quad . \tag{2.3.3}$$

The velocity dependent part of Equation (2.3.3) – the exponential function – is plotted in Figure 2.7 for various normalized distances ξ, where

$$\xi := \frac{\Delta z}{v_{th}\tau} \quad . \tag{2.3.4}$$

The curve $\xi = 0$ represents the initial distribution in the heating region given in Equation (2.3.2). At $\xi > 0$ a hump appears in velocity space. It has a maximum at

$$v_{\max} = \xi^{1/3} v_{th} \quad . \tag{2.3.5}$$

The evolving particle beam is simply an effect of spatial dispersion or, plainly, of fast particles arriving first. The average velocity increases with distance at the expense of beam density. The beam amplitude decreases, since the larger ξ, the earlier in the heating event the particles have originated. The gap at $v = 0$ for $\xi > 0$ expresses that the slowest particles have not yet arrived.

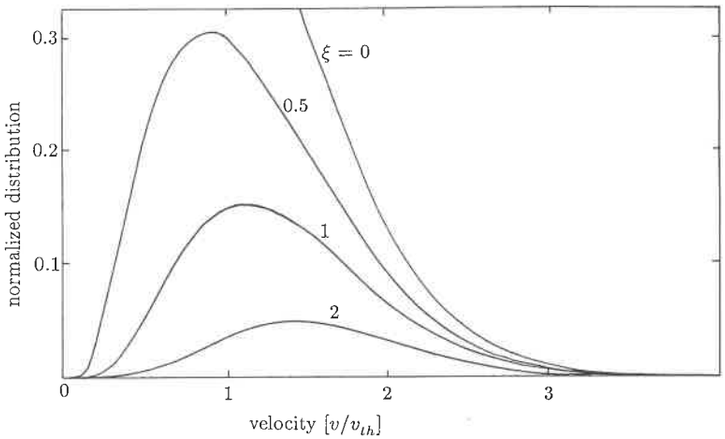

Fig. 2.7. Particle velocity distributions due to a local heating at $\xi = 0$ for various distances ξ from the heating region at any given time $t > 0$.

The simple model lacks many problems encountered in reality. Equation (2.3.1) obviously cannot describe a situation where forces act on the particles. Particle conservation in the presence of electromagnetic forces is expressed by the Boltzmann equation (1.4.11). It can be shown (Exercise 2.3) that Equation (2.3.1) follows from the Boltzmann equation under simplifying conditions. There are two major shortcomings of the simple model, which are briefly mentioned here and which will later be discussed in greater detail:

- Most importantly, an electric field builds up if the evaporating particles carry a charge. The electric field decelerates the particles of the beam and accelerates background electrons to form a *return current*. In the absence of friction (collisions) between background electrons and ions, the electric field is minute, and return current and beam current cancel each other. For large beam currents the frictional loss of the return current becomes an important energy drain of the beam.
- If the peak velocity, $v_{\max}$, of the beam exceeds about three times the thermal velocity of the ambient population, interactions of beam particles with Langmuir waves come into play (Section 5.2). Kinetic particle energy is transferred to oscillating electric fields and substantial energy is lost. Beam-wave interactions have received great interest since electromagnetic emission of the enhanced waves has been observed in solar radio bursts (Section 5.1).

We note that particle beams, as developed in this section, constitute an energy loss of the hot region not included in first-order heat transfer. First-order thermal conductivity is calculated from small deviations of a Maxwellian distribution in the presence of a temperature gradient. Collisionless particles can shorten the cooling time far below first-order calculations.

2.4. Debye Shielding

Up to now we have singled out a particle and calculated its orbit, neglecting interactions with other particles. In this and the following section we consider two fundamental *collective properties* of a plasma. They are both consequences of the presence of free charges of opposite sign.

How do the other particles react to the presence of a charge? Let us calculate the disturbance using classical statistics (see Fig. 2.8). In thermodynamic equilibrium the kinetic particle energy ε is distributed according to Maxwell (Eq. 2.3.2),

$$f_0(\varepsilon) = \frac{n_0}{k_B T} \exp(-\varepsilon/k_B T) \quad . \tag{2.4.1}$$

Now we introduce into the plasma a particle (referred to as the 'test particle') with charge Q creating a potential $\Phi(r)$. If another particle ('field particle') with mass m and charge q approaches the first particle, its total energy is conserved. It remains at the value ε_∞ it had at large distances,

$$\varepsilon + q\Phi(r) = \varepsilon_\infty = \text{const} \quad . \tag{2.4.2}$$

The energy distribution of the field particles also remains constant, but now kinetic and potential energy have to be summed. The energy distribution for field particles with charge q becomes

$$f(\varepsilon, r) = \frac{n_0}{k_B T} \exp[-(\varepsilon + q\Phi)/k_B T] \quad . \tag{2.4.3}$$

The density is given by the normalization

$$n(r) = \int_0^\infty f(\varepsilon, r) d\varepsilon = n_0 \exp(-q\Phi(r)/k_B T) \quad . \tag{2.4.4}$$

Equation (2.4.4) describes how the density of the undisturbed field particles, n_0, is modified by the potential of the test particle. Elementary electrostatics relates Φ to the electric charge density ρ^* by Poisson's equation,

$$-\nabla^2 \Phi = \nabla \cdot \mathbf{E} = 4\pi\rho^* \quad . \tag{2.4.5}$$

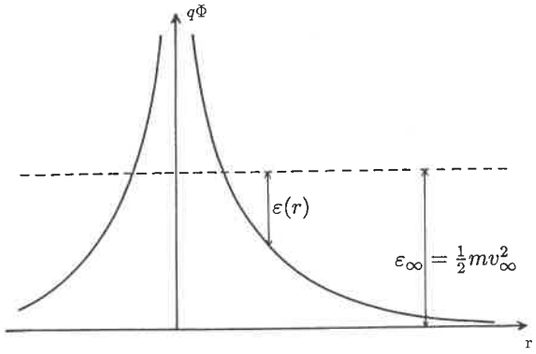

Fig. 2.8. A field particle with charge q experiences the potential Φ of the test particle and (assuming the same sign of the two charges) loses kinetic energy. The total energy of the field particle (dashed line) is conserved.

The charge density ρ^* has been defined in Equation (1.4.6) and is given by the sum over all species α,

$$\rho^* = \sum_\alpha q_\alpha n_\alpha \quad . \tag{2.4.6}$$

As an example we now look at a hydrogen plasma with equal electron and proton temperatures. The undisturbed electron density equals the proton density. Now we disturb this equilibrium with the test charge. Using Equation (2.4.4) and $\rho^* = -e\ n_e + e\ n_p$, the charge density becomes

$$\rho^* = e n_0 [\exp(-e\Phi/k_B T) - \exp(+e\Phi/k_B T)] \quad . \tag{2.4.7}$$

A Taylor expansion of the exponential for $e\Phi/k_B T \ll 1$ in the region of interest immediately yields for Equation (2.4.5)

$$\nabla^2 \Phi = 2 \frac{4\pi n_0 e^2}{k_B T} \Phi \quad . \tag{2.4.8}$$

It is easy to generalize Equation (2.4.8) for a plasma of composition different from hydrogen. $\sum_\alpha Z_\alpha^2 n_\alpha$ then takes the place of $2n_0$, where the sum is over all particle species α. Equation (2.4.8) is a second-order differential equation in Φ. It can be solved in spherical coordinates by trying the form $\Phi(r) = g(r)/r$, and yields

$$\Phi(r) = \frac{a}{r} \exp(-\sqrt{2} r/\lambda_D) \quad , \tag{2.4.9}$$

where $a \approx Q$ follows from the boundary condition on the test charge (assuming this charge to reside on a sphere with radius r_0 and $r_0^2 \ll \lambda_D^2$). In Equation (2.4.9) we have defined the 'Debye-Hückel shielding distance', λ_D, usually termed the *Debye length* for short. It is one of the characteristic lengths in a plasma and amounts to

$$\lambda_D := \sqrt{\frac{k_B T}{4\pi\ n_0 e^2}} = 6.65 \sqrt{\frac{T}{n_e}} \quad \text{[cm]} \ , \tag{2.4.10}$$

where T is in K, and the electron density n_e is in cm^{-3}. A fully ionized multicomponent plasma with solar abundances (27% helium by mass) has been assumed for the numerical expression in Equation (2.4.10).

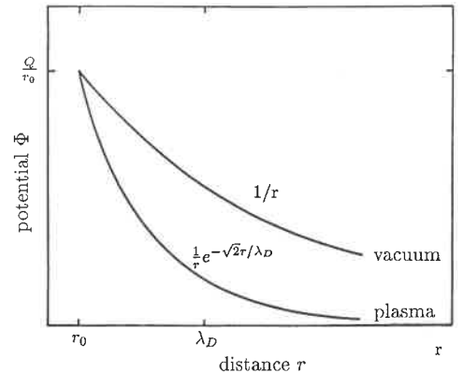

Fig. 2.9. The electric potential of a test charge Q is reduced by the ambient plasma. Here the positive test particle is shielded by field particles of negative charge and by a reduced number of ions in its vicinity.

Equation (2.4.9) means that the electric force of a charge is limited in a plasma to about the Debye length. Particles with opposite charge slightly predominate in its environment, and neutralize its effect (see Fig. 2.9). Only particles separated by less than about λ_D feel the test charge. Of course, the test charge can be any arbitrary particle, and the conclusion is more general: only particles within λ_D are directly influenced by each others' electric fields. The limitation of the direct influence of a charge has far reaching consequences and makes the behavior of a plasma entirely different, for example, from a cluster of gravitationally interacting stars. Since gravitational attraction is not shielded by repulsive forces, it is unlimited in its reach.

With $Q = e$ and $r_0 \ll \lambda_D$ our approximation of Equation (2.4.7) at $r \geq \lambda_D$ is satisfied with

$$\frac{4\pi}{3} n_0 \lambda_D^3 \gg 1 \quad . \tag{2.4.11}$$

The left-hand side is the number of particles in a sphere of radius λ_D (termed the *Debye sphere*) in the undisturbed plasma. It is intuitively clear that this number must exceed unity, as required in Equation (2.4.11), to make Debye shielding work. Assumption (2.4.11) is called the *plasma approximation*.

Debye shielding is usually very efficient in a plasma. For example, in a corona with $n_0 = 10^8 \text{cm}^{-3}$ at a temperature $T = 10^6$ K, $\lambda_D \approx 0.7$ cm; and the number of particles in the Debye sphere is about 10^8, amply justifying our condition (2.4.11).

This process also provides an effective mechanism to prevent local charge accumulation. A concentration of charges of one sign (say electrons) in a region of a plasma would create local electric fields, acting toward the restoration of homogeneity. For $e\Phi \ll k_B T$ the effect of the electric field on the velocity of the field particles is small. The Debye shield builds up mostly by thermal motion: some particles (with opposite charge) remain near the test charge slightly longer, while others (with the same sign of charge) pass by a bit faster. Charge inhomogeneity, as introducing an additional charge, is eroded in this way within a thermal propagation time.

2.5. Charge Oscillations and the Plasma Frequency

In addition to spatial shielding, the plasma species of opposite signs can also lead to charge oscillations around the homogeneous equilibrium discussed in the previous section.

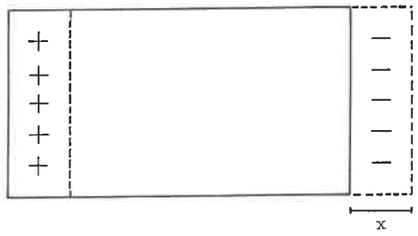

Fig. 2.10. In a 'thought experiment' the electrons are shifted to the right (dashed boundary) and released to oscillate at the plasma frequency.

We perform the following 'thought experiment' drawn in Figure 2.10: The electrons of a plasma are moved slightly to the right by a distance x. Ions are assumed to be fixed (or infinitely inert). This produces a volume $\mathcal{V} = Fx$ to the right where only electrons exist, and an equal volume to the left where only ions remain. Let the number density of electrons in $\mathcal{V}$ be n_e. The electric field produced by this artificial charge separation is given by a simple integration of Poisson's equation (2.4.5). Neglecting edge effects, the problem is one-dimensional and yields, as for an infinitely extended capacitor,

$$E = 4\pi e n_e x \quad . \tag{2.5.1}$$

Now we release the electrons and they are accelerated in the negative x-direction by the electric force. Using Equation (2.5.1) and neglecting thermal motions and collisions,

$$\ddot{x} = -\frac{eE}{m_e} = -\frac{4\pi e^2 n_e}{m_e} x := -(\omega_p^e)^2 x \quad , \tag{2.5.2}$$

where m_e is the electron mass. A characteristic frequency is defined in Equation (2.5.2):

$$\omega_p^e := \left(\frac{4\pi e^2 n_e}{m_e}\right)^{1/2} = 2\pi \cdot 8.977 \cdot 10^3 \sqrt{n_e} \quad \text{[Hz]}. \tag{2.5.3}$$

The solution of Equation (2.5.2),

$$x = a \cos(\omega_p^e t + b) \quad , \tag{2.5.3}$$

describes the restoring motion of the electrons, their overshooting of the equilibrium position ($x = 0$), and oscillation. It is the eigenmode of charge oscillations of electrons around infinitely inert ions. Its frequency, ω_p^e, is called the *electron plasma frequency*. Here we have derived it under very artificial conditions (which however contain and show the essence). We shall later encounter it again in various, more general circumstances (Sections 4.2 and 5.2). We shall find more eigenmodes due to the gyration of charged particles in a magnetic field or due to a particle beam. They are fundamental plasma properties.

In Section 2.4 we mentioned the elimination of charge inhomogeneities by thermal motion and Debye shielding. To avoid this problem in the above experiment, we have to require that the separation of inhomogeneities is larger than the thermal diffusion per oscillation period. This condition amounts to

$$\lambda > 2\pi \frac{v_{te}}{\omega_p^e} = 2\pi \lambda_D \quad . \tag{2.5.5}$$

Equation (2.5.5) suggests that the wave vector $k := 2\pi/\lambda$ of a space-charge wave has to satisfy $k < 1/\lambda_D$, a result that will be derived in a different way in Section 5.2. The identity relation between the fundamental plasma parameters v_{te}, ω_p^e, and λ_D in Equation (2.5.5) simply follows from the definitions (2.4.10) and (2.5.3). It reveals that Debye shielding is an equilibrium between thermal motion (expressed by v_{te}) and electric acceleration ($e^2 n/m$, implied by ω_p^e). The time to establish plasma shielding, $2\pi\lambda_D/v_{te}$, is the electron plasma period.

2.6. Collisions

So far we have neglected interactions between single particles. What is the range of applicability of this approximation? In addition to particle orbits, collisional interactions are also of interest in the broader context of a gas being not in thermodynamical equilibrium. Collisions are likewise important for the thermalization of a super-thermal population or a high energy tail of some particle species, as well as the transport coefficients, such as resistivity, conductivity, or viscosity in some steady non-equilibrium state.

The concept of particle collisions in a plasma is by far the most complex introduced in this chapter and deserves careful study. The word 'collision' generally evokes an image like that of two billiard balls bumping against each other. While not in touch, there is no interaction to speak of. During the extremely short time they are pushed against each other, they feel a strong repulsive force, which practically ceases at the moment the two balls are separated from each other. A collision between two charged particles, however, is a very different process since they interact through the long-range Coulomb force. Thus the collision between two charged particles takes place as a motion of the two charges on hyperbolic paths in each other's electric field.

2.6.1. Particle encounters in a plasma

Let us follow a particle, again to be called a 'test particle', moving simultaneously in the fields created by many other particles (the 'field particles') in a plasma. These fields add up to a stochastically changing force on the test particle; and its orbit is rarely a hyperbola, characteristic of a two particle encounter, but a jittery motion. Two test particles with similar, but not identical starting points and initial velocities will, after some time, diverge into completely different directions with different velocities (Figure 2.11).

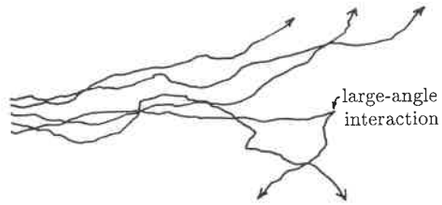

Fig. 2.11. Particles with nearly identical starting conditions diverge in space and velocity due to stochastic collisional interactions.

Collisions in a plasma are therefore of a statistical nature. By a 'collision' we mean the combined effect of a multitude (millions or billions!) of simultaneous interactions with field particles. The collision time in plasma physics is defined as the average time needed for a change of direction, energy, or momentum by an amount to be specified.

It is important for the understanding of collisions in plasmas to distinguish clearly three ranges for field particles at different distances from the test particle. A first dividing line has already been encountered in Section 2.4. The Debye effect shields the test particle from the electric force of charges beyond the Debye length λ_D. We note here that a test particle moving faster than the mean thermal speed of the field particles cannot build up appreciable shielding, being an effect of thermal motion. However, moving in the Debye spheres of field particles, the test particle experiences reduced electric fields.

In fact, particles beyond the Debye length are not without any influence. They may cause a magnetic field or even an electric field that is not completely canceled by shielding (such a situation occurs in electric currents). For such long-range fields the same procedure is adopted as in classical electrodynamics. The local fields of individual charges is neglected in so-called *macroscopic* electric and magnetic fields. The deviations from the smoothed field are *microscopic* fluctuations due to single particles.

The Debye length is about the range of microscopic fields in plasmas, and is a relatively well defined boundary separating two populations of field particles. (*i*) The more distant charges influencing a test particle by macroscopic fields yield smooth test particle orbits, drifts, and oscillations as discussed in Sections 2.1 – 2.3, and 2.5. (*ii*) The charges within the Debye sphere causing microscopic fields lead to stochastic motion, termed *collision*.

A second distinction of field particle distances at the microscopic level is useful to evaluate the process of collision. The criterion is the deflection angle of the path of the test particle in the potential of a given field particle. The deflection is obviously small if the energy of the test particle, $\frac{1}{2}m_T u^2$ (where the subscript T refers to the test particle and u is the velocity relative to the field particle), is large compared to the electric potential, $q_T q_F/r_1$ (where $q_T := Z_T e$ and $q_F := Z_F e$ are the charges of the test particle and the field particle, respectively). The distance of closest approach, r_1, refers to the original orbit of the test particle in the absence of forces. It is generally called the *impact parameter*. The particle is deflected by a small angle only if $r_c < r_1 < \lambda_D$, where

$$r_c := \frac{q_T q_F}{m_T u^2} \tag{2.6.1}$$

is the impact parameter for a 90° deflection. For $r < r_c$ one obtains a large-angle deflection, changing the direction of the orbit by 90° or more by one single encounter. The ratio of small-angle to large-angle interactions varies as the respective impact areas,

$$\frac{\lambda_D^2 - r_c^2}{r_c^2} \lesssim \frac{\lambda_D^2}{r_c^2} \approx \left(\frac{9}{Z_T Z_F}\right)^2 (\frac{4\pi}{3} n_e \lambda_D^3)^2 =: \Lambda^2 \quad . \tag{2.6.2}$$

For the second equation in (2.6.2) we have used Equations (2.6.1) and (2.4.10), and replaced mu^2 by $3k_B T$. The second expression in parentheses is the number of particles in a Debye sphere (derived in Section 2.4) and is assumed to be a large number. Equation (2.6.2) states that small-angle scattering generally outnumbers

large-angle deflections by an enormous factor. It will become clear below (Eq. 2.6.18) that this multitude of distant encounters is about two orders of magnitude more efficient in deflecting the test particle than close binary collisions.

The computational simplification of neglecting large-angle deflections follows immediately. Small, simultaneous interactions become additive, and the scattering of a particle by small-angle deflection is a random walk in angle and velocity.

2.6.2. FOKKER-PLANCK METHOD

The statistical method to describe small-angle deflections has been developed by A.D. Fokker and M. Planck. Let $P(\mathbf{v}, \mathbf{\Delta v})$ be the probability that a test particle changes its velocity $\mathbf{v}$ to $\mathbf{v}+\mathbf{\Delta}v$ in the time interval Δt. Provided that the particle number is conserved, the velocity distribution at time t can be written as

$$f(\mathbf{v},t) = \int f(\mathbf{v}-\mathbf{\Delta}v, t-\Delta t) P(\mathbf{v}-\mathbf{\Delta}v, \mathbf{\Delta}v) d^3\Delta v \quad . \tag{2.6.3}$$

Noting that for small-angle deflections $|\Delta v| \ll |v|$, the product fP in Equation (2.6.3) can be expanded into a Taylor series,

$$\begin{aligned} f(v,t) = \int \{ fP - \Delta t [\frac{\partial}{\partial t} f] P - \mathbf{\Delta v} [\nabla_v fP] \\ + \frac{1}{2} \Delta v_i \Delta v_j [\frac{\partial}{\partial v_i} \frac{\partial}{\partial v_j} fP] + \ldots \} d^3\Delta v \end{aligned} \tag{2.6.4}$$

The Einstein convention has been introduced that the sums over the indices i and j have to be used if they appear together in the numerator and denominator, or as subscripts and superscripts. Since the probability that some transition takes place is unity, P is normalized to

$$\int P d^3\Delta v = 1 \quad . \tag{2.6.5}$$

We define the average velocity change per time interval Δt:

$$\int \mathbf{\Delta v} P d^3\Delta v := < \mathbf{\Delta v} > \quad , \tag{2.6.6}$$

$$\int \Delta v_i \Delta v_j P d^3\Delta v := < \Delta v_i \Delta v_j > \quad . \tag{2.6.7}$$

Exchanging integration and differentiation, the integral in Equation (2.6.4) is readily evaluated. The first term in the integrand cancels with the left hand side of the equation. The remaining terms form the important *Fokker-Planck equation*,

$$\left(\frac{\partial f(\mathbf{v},t)}{\partial t}\right)_{\text{coll}} = \frac{\partial^2}{\partial v_i \partial v_j} \left(f \frac{< \Delta v_i \Delta v_j >}{2\Delta t} \right) - \frac{\partial}{\partial v_i} \left(f \frac{< \Delta v_i >}{\Delta t} \right) \quad . \tag{2.6.8}$$

The possibility of neglecting the higher-order terms in the expansion (2.6.4) is a property of inverse-square law particles having multiple collisions. Equation (2.6.8) shows that the motion of particles in velocity space then can be visualized as a diffusion process. Its right hand side describes the temporal change of a distribution of test particles by multiple, small-angle collision processes. It corresponds to the right hand side of the Boltzmann equation (1.4.11). The first term in Equation (2.6.8) represents the three-dimensional diffusion of the test particle in velocity space; the second term is a friction, slowing down the test particle and moving it radially toward the origin of velocity space.

2.6.3. COLLISION TIMES

The collision time in a plasma is not uniquely defined as in the case of neutral atoms. A charged particle in the Coulomb potential of another particle experiences two effects: (*i*) It is deflected from its initial direction, and (*ii*) it accelerates the field particle. The latter constitutes an energy loss and a drag force (friction) on the motion of the test particle. The relative importance of the two effects depends on the mass ratio of the two particles. If the field particle is much heavier, its acceleration is small, and the direction of motion of the test particle is changed before it loses its energy. The velocity distribution of a set of test particles with the same initial velocity approaches isotropy before the energy is lost. If, on the contrary, the field particle is very mobile, the drag on the test particle slows it down before deflection. The time when a test particle changes its direction is generally different from the time it loses its energy or momentum. Depending on the particular problem, the collision time has to be defined accordingly. Several relaxation times have been introduced by L. Spitzer, some of which we evaluate in the following.

A. *Angular Deflection*

The scattering of a particle from its initial direction by distant encounters is a diffusion process expressed by the first term of the Fokker-Planck equation (2.6.8). It is natural to define the mean *deflection time*

$$t_d := \frac{v^2}{< \Delta v_{\text{perp}}^2 / \Delta t >} \quad , \tag{2.6.9}$$

where $< \Delta v_{\text{perp}}^2 / \Delta t >$ is the average diffusion in velocity perpendicular to the initial velocity $\mathbf{v}$ of the test particle in the time interval Δt. We denote by v_{perp} and v_{par} (needed later) the velocity components perpendicular and parallel, respectively, to the initial velocity. They are generally different from v_z and $v_\perp$, the velocity components relative to the magnetic field. The collision time, as defined in Equation (2.6.9), is the average time in which the test particle is deflected through an angle of order 90°.

The calculation of $< \Delta\mathbf{v} \circ \Delta\mathbf{v} >$ is lengthy but straightforward, and is omitted here. The interested reader is referred to the classical textbooks of plasma physics listed at the end of the chapter. It is based on the simple physical idea that the test particle's velocity changes gradually under the influence of many field particles, whose motions are approximated by straight lines. The electric force on the test particle is given by adding the combined effects of the field particles. To average the effect, the sum is replaced by integration over the distribution in space and velocity. For field particles with an isotropic, Maxwellian distribution, the integral in velocity space reduces to the part $|v_F| < |v_T|$ and yields the error function Ψ and the combination G with its derivative, where

$$\Psi(x) := \sqrt{\frac{2}{\pi}} \int_0^x \exp(-\frac{y^2}{2}) dy \quad , \tag{2.6.10}$$

$$G(x) := \frac{\Psi(x) - x\Psi'(x)}{x^2} \quad . \tag{2.6.11}$$

The limiting values are

$$\lim_{x \to \infty} \Psi(x) = 1 \quad , \tag{2.6.12}$$

and

$$\lim_{x \to \infty} G(x) = \frac{1}{x^2} \quad . \tag{2.6.13}$$

The general result of the integration in velocity space is

$$t_d = \frac{v^3}{A_d[\Psi(v/v_{tF}) - G(v/v_{tF})]} \quad , \tag{2.6.14}$$

where the diffusion constant A_d has been defined by

$$A_d := \frac{8\pi n_F q_T^2 q_F^2 \ln \Lambda}{(m_T)^2} \quad . \tag{2.6.15}$$

Λ is the ratio of the boundaries on the integral over space around the test particle where interactions take place. A finite lower limit of the impact parameter has to be introduced to guarantee approximate rectilinear motions. Since small angle deflections dominate, we put $r_{\min} = r_c$, and Λ is therefore given by Equation (2.6.2). As it enters only as a natural logarithm, the rough approximations of the boundaries are greatly alleviated. For solar abundances and electrons or protons as test particles,

$$\Lambda \approx \begin{cases} 1.24 \cdot 10^4 (T^{3/2}/n_e^{1/2}), & \text{for } T \lesssim 4.2 \cdot 10^5 \text{ K} \quad (2.6.16) \\ 8.0 \cdot 10^6 (T/n_e^{1/2}), & \text{for } T \gtrsim 4.2 \cdot 10^5 \text{ K} \quad (2.6.17) \end{cases}$$

Equation (2.6.17) includes quantum-mechanical effects on electrons at large velocities where r_c falls below the de Broglie wavelength of the particles. For collisions between ions, the classical expression, Equation (2.6.16), should be used. In the solar and stellar coronae and outer envelopes, $\ln\Lambda$ is about 20 and decreases to around 10 in the chromosphere. The theory breaks down for extremely high densities and low temperatures, where Λ approaches unity.

It is instructive to consider the deflection of a fast particle having $v \gg v_{tF}$ (the thermal velocity of the field particles). According to Equations (2.6.12) and (2.6.13), G can then be neglected and $\Psi \approx 1$. The deflection time becomes

$$t_d \approx \frac{1}{\pi n v r_c^2} \frac{1}{8 \ln\Lambda} := t_{ce} \frac{1}{8 \ln\Lambda} \quad , \tag{2.6.18}$$

where $t_{ce} = (\pi n v r_c^2)^{-1}$ is the collision time of close encounters. In the plasmas of interest here, Equation (2.6.18) is consistent with the assumption of the Fokker-Planck method that close encounters can be neglected. Since a test particle feels both electrons and ions, the total deflection time combines the effect of all field particles, and

$$t_d \approx \frac{m_T^2 v_T^3}{8\pi e^4 (n_e + \sum_i Z_i^2 n_i) Z_T^2 \ln\Lambda} \quad . \tag{2.6.19}$$

A useful approximation for a non-relativistic, super-thermal particle with kinetic energy ε_{keV} (in keV) in a fully ionized plasma with solar abundances is

$$t_d = 9.5 \cdot 10^7 \frac{\varepsilon_{\text{keV}}^{3/2}}{n_e} \left(\frac{m_T}{m_e}\right)^2 \frac{1}{Z_T^2} \left(\frac{20}{\ln\Lambda}\right) \quad [\text{s}] \ , \tag{2.6.20}$$

where collisions with both electrons and ions have been taken into account. The deflection time (2.6.20) has been numerically evaluated in Table 2.1 for electrons and protons moving with $v \gg v_{tF}$. We note that this deflection time, *increasing* with velocity in proportion to v^3, is different from neutral atoms and billiard balls (where collision time decreases as $1/v$). The faster a charged particle moves through a plasma, the smaller its frictional drag. It is this property of longevity which makes super-thermal particles a distinct population in some cosmic plasmas.

The magnetic field has been omitted in this discussion. It does not change the basic process of deflection nor the derived collision times. Collisions, however, allow charged particles to diffuse across magnetic field lines. The diffusion is simply caused by random steps of about one gyroradius within a collision time, t_d.

B. *Energy Exchange*

Another collision time, t_{ex}, is related to the energy change between the test particle and the field particles. In analogy to the deflection time we define the *energy-exchange time* by

$$t_{ex} := \frac{\varepsilon^2}{< \Delta\varepsilon^2/\Delta t >} \quad . \tag{2.6.21}$$

This definition is meaningful if the test particle has a velocity of the order of the thermal velocity of the field particles. The energy change then fluctuates in

its sign, and Equation (2.6.21) describes the net effect. Writing the exchange of energy in terms of parallel and perpendicular velocity relative to the initial velocity **v** of the test particle,

$$\Delta\varepsilon = \frac{m}{2}\left\{[(v+\Delta v_{\rm par})^2 + \Delta v_{\rm perp}^2] - v^2\right\} \quad . \tag{2.6.22}$$

After averaging over the statistical ensemble we find in the lowest order of Δ-terms

$$< \Delta\varepsilon^2 > = m^2 v^2 < \Delta v_{\rm par}^2 > \quad , \tag{2.6.23}$$

and, again using the Fokker-Planck method,

$$t_{ex} = \frac{v^2}{4 < \Delta v_{\rm par}^2/\Delta t >} = \frac{v^3}{4A_d G(v/v_{tF})} \quad . \tag{2.6.24}$$

The energy-exchange time is for instance used to determine the time to equalize the temperatures of two plasma species (Exercise 2.5). For infinitely heavy field particles, t_{ex} approaches infinity as the field particles become stationary, the test particle would move in their fixed potential, and collisions are elastic. Equation (2.6.24) becomes unreliable for large v/v_{tF} where secondary terms contribute.

C. *Momentum Loss*

The effects of collisions on macroscopic motions such as friction, viscosity, electric resistance, and wave damping frequently require an evaluation of the average loss of forward momentum. The slowing down of the initial velocity of a test particle is a combination of the frictional forces and deflections by multi-particle interactions. Which effect dominates depends on the mass of the field particles. It is measured by the *slowing-down time*,

$$t_s := -\frac{v}{< \Delta v_{\rm par}/\Delta t >} = \frac{2v(v_{tF})^2}{[1+m_T/m_F]A_d G(v/v_{tF})} \quad . \tag{2.6.25}$$

For $v \gg v_{tF}$ it is proportional to v^3. Contrary to t_{ex}, the slowing-down time is finite for infinitely heavy field particles and is twice the deflection time, since forward momentum loss is dominated by deflection. Nevertheless, the slowing-down time for electron motions close to (or below) the thermal speed of the field particles is different and needs careful evaluation.

D. *Energy Loss*

A very important collision time is the energy loss of a fast particle. At $v_T \gg v_{tF}$, the test particle only loses energy by interactions. The *energy loss time* is defined by

$$t_\varepsilon := -\frac{\varepsilon}{< \Delta\varepsilon/\Delta t >} \quad . \tag{2.6.26}$$

Using Equation (2.6.22), we rewrite it as

$$\frac{1}{t_\varepsilon} = -\frac{2v < \Delta v_{\rm par}/\Delta t >}{v^2} - \frac{< \Delta v_{\rm par}^2/\Delta t >}{v^2} - \frac{< \Delta v_{\rm perp}^2/\Delta t >}{v^2} \quad . \tag{2.6.27}$$

This equation can be expressed in the previously derived terms according to the definitions (2.6.25), (2.6.24), and (2.6.9).

$$\frac{1}{t_\varepsilon} = \frac{2}{t_s} - \frac{4}{t_{\rm ex}} - \frac{1}{t_d} = \frac{A_d}{v^3}\left[(1+\frac{m_T}{m_F})(\frac{v}{v_{tF}})^2 G(v/v_{tF}) - \Psi(v/v_{tF})\right] \quad . \tag{2.6.28}$$

For $v \gg v_{tF}$ it simplifies to

$$t_\varepsilon \approx \frac{v^3 m_F}{A_d m_T} \quad . \tag{2.6.29}$$

Let an electron be the test particle for illustration. Equation (2.6.29) then yields a very long energy loss time for protons as the field particles. The physical reason is again the large inertia of protons, making interactions with them nearly loss-free. Thus the relevant collision partners and field particles are the thermal electrons. For fast electrons, the energy loss time becomes equal to the electron-electron deflection time (Eq. 2.6.14). Also for proton test particle, the much more mobile field electrons absorb most of the collision energy.

Relativistic electrons lose energy within a time of

$$t_\varepsilon^{\rm rel} \approx 1.59 \cdot 10^{12}\,\frac{\varepsilon_{MeV}}{n_e} \quad , \tag{2.6.30}$$

where ε_{MeV} is the particle energy in MeV (Benz and Gold, 1971).

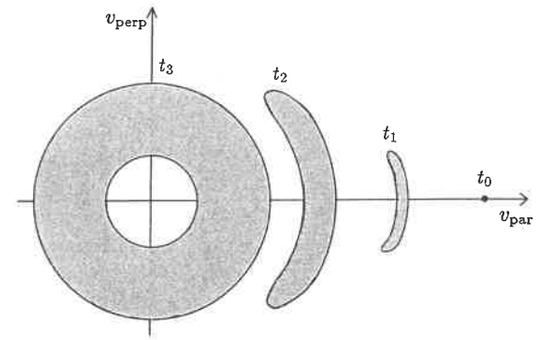

Fig. 2.12. Evolution of the probability distribution of a super-thermal electron due to small-angle scattering starting at t_0 with a velocity $\mathbf{v_0}$. Since energy exchange and friction are slow, changes in direction dominate. After $t_\varepsilon \gtrsim t_s \gtrsim t_d$ the ring distribution contracts toward zero velocity.

E. *Discussion*

How are the different collision times related to each other? As an example, let us follow in time a fast electron (test particle) interacting with field particles. The small-angle deflections by microscopic fields in a plasma scatter the test particle in a stochastic way described by a probability distribution $f_T(\mathbf{x}, \mathbf{v}, t)$ in space and velocity. The distribution is initially a delta function in six dimensions, $\prod_{i=1}^{3} \delta(x_i - x_{0i})\delta(v_i - v_{0i})$, centered at the initial position and velocity. The four collision times derived above indicate how this probability function spreads out, and they suffice for a statistical description of the behavior of a test particle (Figure 2.12). If the electron initially is super-thermal (i.e. $v_T \gg v_{tF}$), pitch-angle scattering predominates. The probability distribution grows only slowly in width parallel to $\mathbf{v}$, since energy-exchange is extremely slow (Eq. 2.6.24). After a time t_d the distribution forms a ring in the ($v_{\rm perp}$-$v_{\rm par}$) plane (about at t_3 in Fig. 2.12), when the forward momentum is also lost. The radius of the ring decreases by energy loss. Energy exchange widens the ring (see Eq. 2.6.23), which finally shrinks toward the compact distribution of the field particles near the origin of velocity space after about t_ε.

Table 2.1. Collision times in seconds for non-relativistic test particles with $v_T \gg v_{tF}$ in a fully ionized hydrogen plasma with solar helium abundance and using cgs units. The values in the table have to be corrected by the factor $20/\ln\Lambda$, being usually of order unity.

test $\rightarrow$	electron	electron	proton	proton
field $\rightarrow$	electrons	ions	electrons	ions
t_d	$3.1 \cdot 10^{-20} \frac{v_T^3}{n_e}$	$2.7 \cdot 10^{-20} \frac{v_T^3}{n_e}$	$1.0 \cdot 10^{-13} \frac{v_T^3}{n_e}$	$9.0 \cdot 10^{-14} \frac{v_T^3}{n_e}$
t_s	$3.1 \cdot 10^{-20} \frac{v_T^3}{n_e}$	$5.4 \cdot 10^{-20} \frac{v_T^3}{n_e}$	$1.1 \cdot 10^{-16} \frac{v_T^3}{n_e}$	$1.0 \cdot 10^{-13} \frac{v_T^3}{n_e}$
t_ε	$3.1 \cdot 10^{-20} \frac{v_T^3}{n_e}$	$6.2 \cdot 10^{-17} \frac{v_T^3}{n_e}$	$5.7 \cdot 10^{-17} \frac{v_t^3}{n_e}$	$1.1 \cdot 10^{-13} \frac{v_T^3}{n_e}$

It is evident from Table 2.1 that a super-thermal particle (electron or proton) is deflected by ions equally well as by electrons (except for a small difference due to field particle densities converted into n_e). This is not true for energy loss. An electron is slowed down twice as much by thermal electrons as by ions, and an ion is retarded almost exclusively by the friction of electrons. This difference between electron and ion slow-down has a simple explanation. A beam of super-thermal electrons is decelerated also by loss of directed momentum, not only by energy loss of individual particles. Thus super-thermal electrons are decelerated in forward momentum and deflected at similar rates. Ions are slowed down faster than deflected.

In conclusion, we note that the collision times of a charged particle in a plasma increase with velocity to a power of 3 or 5. It is opposite to billiard balls (or neutral atoms), in which collision time decreases with velocity. This unusual property

is specific to the inverse-square law of particle interaction and has far-reaching consequences in astrophysics: Once charged particles are accelerated, they keep their energy much longer than the collision time of the thermal background particles. Energetic particles may exist long after their acceleration and can serve as indicators of violent processes in the past, like the smoke of a gun. As an example, we just mention cosmic rays in interstellar space, which – once accelerated in a supernova or a stellar flare – have t_ε easily exceeding 10^9 years. Nuclear collisions, following a different law, effectively reduce this time.

F. *Thermal Collision Times*

The different collision times become practically identical for a test particle moving at the thermal velocity and interacting with its own species. Deflection and energy exchange occur at similar rates. This *thermal collision time* – also called self-collision time – is a characteristic time of a plasma species rather than of a single particle. Its value generally is taken as t_d evaluated at the root mean square thermal velocity in three dimensions, $(3k_BT/m)^{1/2}$, and amounts to

$$t_t = \frac{v^3}{0.714 A_d} \approx \frac{0.267}{\ln\Lambda} \frac{T^{3/2}}{Z^4 n} \left(\frac{m}{m_e}\right)^{1/2} \quad [\mathrm{s}] \ , \tag{2.6.31}$$

where Z is the charge of the particles in units of e, the elementary electron charge, T is in K, n in cm^{-3}, and Λ has to be evaluated from Equation (2.6.16) or (2.6.17). The thermal collision time sets the time scale in which the bulk of a plasma regains thermal equilibrium after a disturbance. We note that (*i*) this takes $(m_p/m_e)^{1/2}$ longer for protons than for electrons, and (*ii*) that for 20 keV electrons, to give an example, t_ε is more than three orders of magnitude larger than t_t for thermal electrons at 10^6 K.

Waves that include oscillating electrons (an example was given in Section 2.5) are damped by the collisional randomization of electron momentum on ions. The process occurs within the thermal *electron-ion collision time*, $t_{e,i}$, calculated from the forward momentum loss (Eq. 2.6.25),

$$t_{e,i} = 1.907 \cdot 10^{-2} \frac{T^{3/2}}{\sum_i Z_i^2 n_i} \left(\frac{20}{\ln\Lambda}\right) \quad [\mathrm{s}] \ . \tag{2.6.32}$$

The ions are the field particles. For a fully ionized plasma with solar abundances $\sum_i Z_i^2 n_i \approx 1.16\ n_e$.

Exercises

2.1: Particles moving along a curved magnetic field experience a drift due to their inertia. Calculate the centrifugal drift (Eq. 2.1.29) by defining a 'centrifugal force',

$$\mathbf{F}_c := \frac{m v_z^2}{R_c^2} \mathbf{R}_c \quad , \tag{2.6.33}$$

where R_c is the curvature radius of the magnetic field.

2.2: Calculate the bounce period (Eq. 2.2.4) of a particle orbiting in a symmetric magnetic loop having a parabolic form: $B = B_0(1 + s^2/H_B^2)$, where s is the distance from the top.

2.3: Prove that Equation (2.3.1) is consistent with the Boltzmann equation (1.4.11) in the absence of collisions and other forces.

2.4: Calculate the distance after which a beam evolving out of a hot Maxwellian distribution exceeds three times the mean thermal velocity, v_{tc}, of the cold population, the approximate threshold for instability. Assume $v_{th}/v_{tc} = 10$, $T_c = 2 \cdot 10^6$K, and $\tau = 1$s, values typical for solar type III radio bursts.

2.5: Prove that the equilibration time to equalize the temperatures of two plasma species T and F defined by

$$t_{eq} := \mid T_F - T_T \mid (dT_T/dt)^{-1} \tag{2.6.34}$$

amounts to

$$t_{eq} = \frac{m_T m_F}{8\sqrt{2\pi} q_T^2 q_F^2 n_F \ln\Lambda} \left(\frac{k_B T_T}{m_T} + \frac{k_B T_F}{m_F} \right)^{3/2} . \tag{2.6.35}$$

[*Hint:* Calculate $< \Delta\varepsilon_T >_F$ and average over velocity of species T.] As an example evaluate t_{eq} for the solar wind, where the electron temperature usually exceeds the ion temperature. How long would it take to relax the observed difference near Earth between electrons (say $T_e = 10^5$ K) and protons ($T_p = 3 \cdot 10^4$ K) in the solar wind if the density ($n_e = 5$ cm^{-3}) did not change?

Further Reading and References

Adiabatic invariants and drifts

Schmidt, G.: 1979, *Introduction to High Temperature Plasmas* (2nd edition), Chapter 2, Academic Press, New York.

Collisions

Spitzer, L.: 1962, *Physics of Fully Ionized Gases*, Interscience Publ., New York.

Schmidt, G.: 1979, *op.cit.*, Chapter 11.

Emslie, A.G.: 1978, 'The Collisional Interaction of a Beam of Charged Particles with a Hydrogen Target of Arbitrary Ionization Level', *Astrophys. J.* **224**, 241.

Petrosian, V.: 1985, 'Directivity of Bremsstrahlung Radiation from Relativistic Beams and the Gamma Rays from Solar Flares', *Astrophys. J.* **299**, 987.

References

Benz, A.O., and Gold, T.: 'Magnetically Trapped Particles in the Lower Solar Atmosphere Directivity', *Solar Phys.* **21**, 157.

Boström, R., Koskinnen, H., and Holback, B.: 1987, 'Low-Frequency Waves and Small-Scale Solitary Structures Observed by Viking', *ESA SP* **275**, 185.